Phonon-assisted transport in van der Waals heterostructure tunnel devices

A. M'foukh[1], J. Saint-Martin[1], P. Dollfus[1], M. Pala[1]

[1]Université Paris-Saclay, Centre de Nanosciences et de Nanotechnologies, CNRS, F-91120 Palaiseau, France, adel.mfoukh@c2n.upsaclay.fr

1. Abstract

In this work, we present a first-principles study of quantum transport in tunnel FETs based on van der Waals (vdW) heterostructures of transition metal dichalcogenides (TMDs). We focus on 1T-$HfSe_2$ and 1T-SnS_2 monolayers to construct a vertical heterostructure with a type-II band alignment. By including dissipative effects due to the electron-phonon interaction, we show that vdW tunnel FETs are highly sensible to the phonon coupling due to polar optical phonons present in TMDs which results in an increased sub-threshold swing (SS) and reduced ON-current. However, vdW TFETs are still able to provide high ON-current values due to the inversion of CB and VB at high V_{GS} and high inter-valley tunneling.

2. Introduction

The tunnel FET (TFET) paradigm continues to attract interest being able to reach a sub-thermionic behavior in opposition to the MOSFET. However, the ON-current of TFETs based on single 2D materials remains small [1]. In this context, van der Waals heterostructures represent a promising platform to look for future electron devices due to high drive currents and steep swings achievable with vertical tunneling architectures [2-4]. One of the main scattering mechanisms present in this type of materials and devices is electron-phonon scattering that must be carefully taken into account for a realistic estimation of device performance. In this work, we propose a first-principles study of electron transport properties of tunnel FETs based on vdW heterojunctions as sketched in Figure 1.

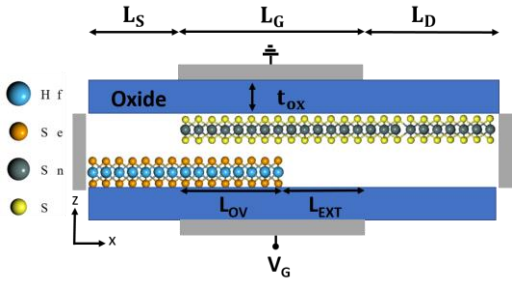

Figure 1. VdW TFET sketch with $L_{S/D}$=8nm, L_G=15nm, L_{OV}=10nm, L_{EXT}=5nm.

In order to rigorously take into account quantum phenomena ruling the physics of this device with an ab initio approach, the calculations were performed by means of a home-made code that couples density functional theory (DFT) with non-equilibrium Green's function formalism [5]. We focused on 1T-$HfSe_2$ and 1T-SnS_2, two transition metal dichalcogenides (TMDs) with a type II band alignment [6], actually close to a type III. This kind of heterostructure is expected to be achieved by exfoliating each material and manually stacking them [7] or by CVD [8]. Their bandstructures

resulting from DFT calculations are plotted in Figure 2. A band inversion between the VB of $HfSe_2$ and the CB of SnS_2 can be achieved by imposing a vertical electric field. Also, it can be noticed the small degree of hybridization between the two materials, which arises from the long-range van-der Waals forces and which avoids Fermi level pinning at the interface.

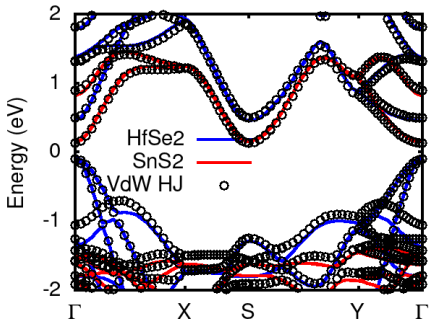

Figure 2. Band structures of the monolayers of 1T-SnS_2 and 1T-$HfSe_2$ and their vdW heterostructure.

3. Method

In this work, we made use of the plane-wave Hamiltonians computed with the DFT solver Quantum ESPRESSO [9]. We adopted norm-conserving pseudopotentials based on the Perdew-Burke-Ernzerhof (PBE) [10] exchange-correlation functional. Van der Waals interactions were considered in the calculations with non-local van der Waals functional vdW-DF3 [11]. The unit cell of each material has been relaxed and the calculation of band structures was performed with a kinetic energy cut-off of 60 Ry. 1T-SnS_2 is found to be a semiconductor with a bandgap around 1.64eV with a lattice parameter of 3.7Å, which is consistent with literature. For 1T-$HfSe_2$, DFT calculation leads to a bandgap of 0.53eV and an atomic lattice of 3.752Å. These two materials are thus lattice matched and can form a heterostructure with a strain smaller than 1%. In order to combine DFT Hamiltonian with quantum transport calculation, the Hamiltonian is projected on a reduced basis composed of unit-cell restricted Bloch functions [5].

The transport properties are computed within the non-equilibrium Green's function formalism with a home-made solver based on the method presented in [5], where the kinetic equations for the Green's functions are solved self-consistently with the 3D Poisson equation to obtain an accurate electrostatic description of the system. To take into account the electron scattering with acoustic and optical phonons, we considered DFT and density functional perturbation theory (DFPT). Phonon scattering has been included in the NEGF code by considering local self-energies within the self-consistent Born approximation (SCBA) [12] where the phonon bath is kept at equilibrium. For acoustic phonon scattering at room temperature, the elastic approximation can be used, namely considering $E \pm \hbar\omega_q \approx E$, where ω_q is the phonon frequency at wave vector q. Optical phonon modes are considered dispersion-less. The electron-phonon matrix elements M_q for acoustic and optical phonons were described by deformation potential as:

$$\left|M_q\right|^2_{ac} = \frac{D^2_{ac}\hbar q}{2\rho v_s} \text{ and } \left|M_q\right|^2_{op} = \frac{\hbar D^2_{op}}{2\rho\omega_q} \quad (1)$$

Where ρ is the mass density of the 2D material, and v_s is the sound velocity. For acoustic phonon, the deformation potential was calculated from DFT as follows [13]:

$$D_{ac} = \frac{\partial E_{C/V}}{\partial \delta} \quad (2)$$

Where $E_{C/V}$ is the conduction or valence band energy for electron or hole respectively and δ is the biaxial strain applied to the unit cell.

In this system, the coupling between the electrons and the longitudinal optical (LO) phonon mode is strong and dominates with respect to non-polar optical phonons. Here, the Fröhlich interaction of polar phonon was described through a deformation potential derived from the scattering rate computed from a 2D model with DFPT inputs [14]. In this model, the dielectric environment was also taken into account in the scattering rate calculation. The deformation potential was obtained by using the self-energy relaxation time approximation that is expressed as:

$$\frac{D_{op}^2}{\rho\omega} \frac{\sqrt{m_x m_y}}{2\pi\hbar^2} = \frac{1}{\tau_{op}} \quad (3)$$

Where m_x and m_y are the effective masses along x and y direction, respectively.

4. Results

The architecture of the van der Waals tunnel FET under study is illustrated in Figure 1. The source is composed of p-doped $HfSe_2$ monolayer, the drain of n-doped SnS_2 monolayer and the channel of the vdW heterojunction. Two gates cover the channel region where the SnS_2 is undoped and the $HfSe_2$ that is p-doped with the same doping concentration of the source $N_A=1.0\times10^{13}$ cm^{-2}. The drain is n-doped with a concentration of $N_D=1.0\times10^{13}$ cm^{-2}. Recent works suggest that it is possible to spatially control the doping in 2D material with a chemical doping [15-16]. Concerning the electric control of the devices, a high-κ oxide with a dielectric constant of 25 (similar to HfO_2) and a thickness of 3.2 nm have been chosen to obtain an equivalent oxide thickness (EOT) of 0.5 nm. One of the gate is grounded in order to control the electric field generated by the other gate in the vdW heterostructure and thus efficiently modulate the bandgap in this region. The gates are extended over the drain region material in order to reduce current in off state [4]. Last but not least, a work function difference between the two gates of 0.7eV is chosen to achieve the band inversion at the same time as the band-to-band tunneling between the source and the 1T-SnS2 monolayer of the channel. Electron-phonon coupling and phonon parameters are summarized in TABLE 1.

TABLE I. PHONON AND ELECTRON-PHONON COUPLING PARAMETERS

	D_{AC} (eV)	$\hbar\omega_{POP}$ (meV)	$1/\tau_{POP}$ (10^{11}s^{-1})	D_{POP} (10^8eV.cm^{-1})
1T-SnS_2	5.47	30	6.7	3.7
1T-$HfSe_2$	2.49	25	8.9	2.7

We found that the electron-phonon coupling is responsible of numerous phenomena degrading the current control of the device, as shown in Figure 3, where we plot the results of calculations with different scattering rates of the polar optical phonon scattering τ_{POP} to emphasize its impact.

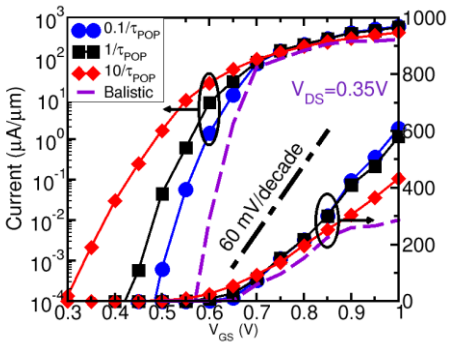

Figure 3. Transfer characteristics for different scattering rates and V_{DS}=0.35V.

A first remark about the I-V curves is that the inclusion of electron-phonon scattering induces always an increase of the drain current with respect to the ballistic calculation, even in ON state. This phenomenon can be explained with the contribution of inter-valley transmission mediated by phonons from the valence band (VB) of $HfSe_2$ in Γ to the conduction band (CB) of SnS_2 in S (see Figure 2). This is illustrated in Figure 4 and Figure 5, showing the current spectrum in the ON state for two different lateral wave vectors k_y. In the k_y=0 case, the charge flow is localized in the source region composed of $HfSe_2$, while in the $k_y=0.5\times 2\pi/a_y$ case, in the channel region made of the SnS_2. We remark that this phenomenon cannot be observed with a mere ballistic simulation.

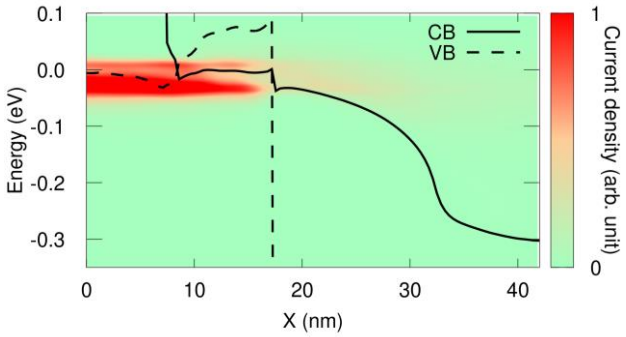

Figure 4. Contour plot of the current spectrum. CB (solid line) and VB (dashed line) profiles along the transport direction for V_{GS} =0.35 V and $k_y=0\times 2\pi/a_y$.

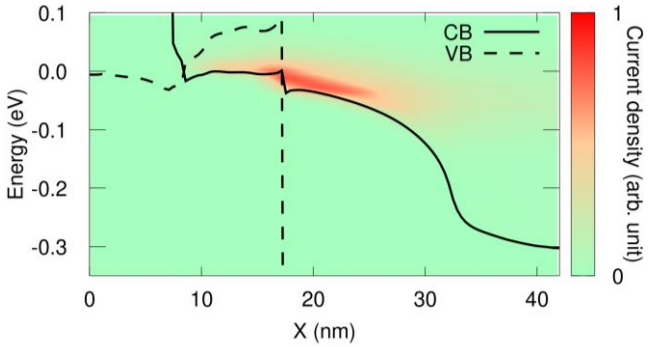

Figure 5. Contour plot of the current spectrum. CB (solid line) and VB (dashed line) profiles along the transport direction for V_{GS} =0.35V and $k_y=0.5\times 2\pi/a_y$.

Figure 6 shows the current spectrum in the OFF state and illustrates the importance of phonon absorption mechanism in the vdW region that, in addition with the small bandgap of the vdW heterostructure, produces a significant degradation of the sub-threshold slope.

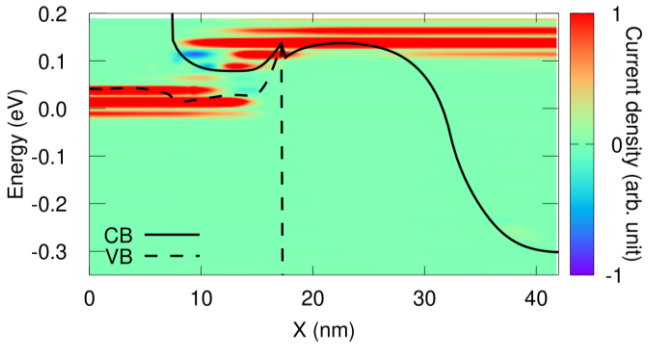

Figure 6. Current spectrum and CB (solid line) and VB (dashed line) profiles along the transport direction for V_{GS} =0V.

Figure 7 shows the current spectrum in the ON state where band inversion is achieved in the vdW region. A further resistive effect due to the phonon emission in the drain is visible and explains the decrease of the ON-state current as a function of the polar optical phonon coupling visible in Figure 3.

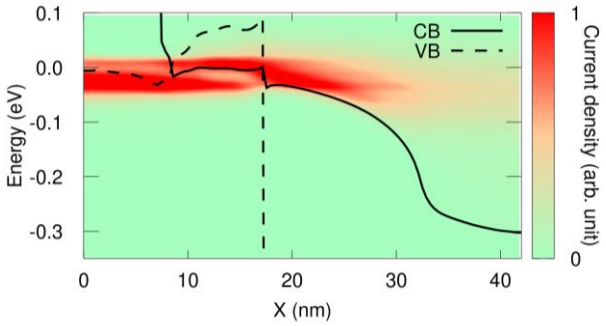

Figure 7. Current spectrum and CB (solid line) and VB (dashed line) profiles along the transport direction for V_{GS} =0.35V.

5. Conclusion

A theoretical study of dissipative transport in vdW TFETs has been addressed thanks to a full-ab-initio model. The results suggest that vdW TFETs are significantly affected by phonon scattering due to the large coupling of electrons with polar phonons. However, they remain a promising option for the next generation electronics due to the high current around 580μA/μm and a SS of 26mV/dec reached at low voltage with phonon coupling.

Acknowledgements

Financial support from the ANR projects “2D-on-demand” (n. ANR-20-CE09-0026-02) and “Tunne2D” (n. ANR-21-CE24-0030-03) is gratefully acknowledged.

References

[1] Á. Szabó, C. Klinkert, D. Campi, C. Stieger, N. Marzari and M. Luisier, "Ab Initio Simulation of Band-to-Band Tunneling FETs With Single- and Few-Layer 2-D Materials as Channels," *IEEE Transactions on Electron Devices*, vol. 65, no. 10, pp. 4180-4187, 2018.

[2] A. Afzalian, E. Akhoundi, G. Gaddemane, R. Duflou and M. Houssa, "Advanced DFT–NEGF Transport Techniques for Novel 2-D Material and Device Exploration Including HfS_2/WSe_2 van der Waals Heterojunction TFET and WTe_2/WS_2 Metal/Semiconductor Contact," *IEEE Transactions on Electron Devices*, vol. 68, no. 11, pp. 5372-5379, 2021.

[3] D. Logoteta, J. Cao,M. Pala, P. Dollfus, Y. Lee, and G. Iannaccone “Cold-source paradigm for steep-slope transistors based on van der Waals heterojunctions.” *Physical Review Research,* vol.2 (4), 2020.

[4] J. Cao, D. Logoteta, S. Ozkaya, B. Biel, A. Cresti, M. G Pala, and D. Esseni. “Operation and Design of Van Der Waals Tunnel Transistors: A 3-D Quantum Transport Study.” *IEEE Transactions on Electron Devices* , vol. 63, no. 11, pp. 4388–4394, 2016.

[5] M. G. Pala, P. Giannozzi, and D. Esseni, “Unit cell restricted bloch functions basis for first-principle transport models: Theory and application,” Phys. Rev. B, vol. 102, p. 045410, 2020.

[6] S. Su, P. Das, S. Ge, and R. K Lake. “Graphene Contacts to a HfSe2/SnS2 Heterostructure.” *The Journal of Chemical Physics* , vol. 146, no. 6, pp. 64701–064701, 2017.

[7] X. Zhou, X. Hu, S. Zhou, H. Song, Q. Zhang, L. Pi, L. Li, H. Li, J. Lü, and T. Zhai. "Tunneling Diode Based on WSe2/SnS2 Heterostructure Incorporating High Detectivity and Responsivity." *Advanced Materials (Weinheim)* , vol. 30, no. 7, pp. 1703286, 2018.

[8] J. Zribi, L. Khalil, B. Zheng, J. Avila, D. Pierucci, T. Brulé, . . . A. Ouerghi, "Strong Interlayer Hybridization in the Aligned SnS2/WSe2 Hetero-Bilayer Structure." *NPJ 2D Materials and Applications* , vol. 3, no. 1, 2019.

[9] P. Giannozzi, S. Baroni, N. Bonini, M. Calandra, R. Car, C. Cavazzoni, . . . R. Wentzcovitch, "QUANTUM ESPRESSO: a Modular and Open-Source Software Project for Quantum Simulations of Materials." *Journal of Physics. Condensed Matter* , vol. 21, no. 39, p. 395502, 2009.

[10] J. Perdew, K. Burke, and M. Ernzerhof "Generalized Gradient Approximation Made Simple [Phys. Rev. Lett. 77, 3865 (1996)]." *Physical Review Letters* , vol. 78, no. 7, p. 1396, 1997.

[11] D. Chakraborty, K. Berland, and T. Thonhauser, "Next-Generation Nonlocal Van Der Waals Density Functional." Journal of Chemical Theory and Computation, vol. 16, no. 9, pp. 5893–5911, 2020.

[12] H. Haug and A.-P. Jauho, Quantum kinetics in transport and optics of semiconductors (Springer, 2008).

[13] R. Resta, "Deformation-Potential Theorem in Metals and in Dielectrics." Physical Review. B, Condensed Matter, vol. 44, no. 20, pp. 11035–11041, 1991.

[14] T. Sohier M. Calandra, and F. Mauri."Two-Dimensional Fröhlich Interaction in Transition-Metal Dichalcogenide Monolayers: Theoretical Modeling and First-Principles Calculations." Physical Review. B, Condensed Matter and Materials Physics, vol. 94, no. 8, 2016.

[15] Y. Gong, H.Yuan, C. Wu, P. Tang, S. Yang, A. Yang, . . . Y. Cui. "Spatially Controlled Doping of Two-Dimensional SnS 2 through Intercalation for Electronics." *Nature Nanotechnology* , vol. 13, no. 4, p. 294, 2018.

[16] T. Eknapakul, I. Fongkaew, S. Siriroj, W. Jindata, S. Chaiyachad, S. Mo, . . . W. Meevasana, "Direct observation of strain-induced orbital valence band splitting in HfSe2 by sodium intercalation. " *Physical Review. B, Condensed Matter* , vol. 97, no. 20, 2018.